Combined effect of simplicial complexes and interlayer interaction: An example of information-epidemic dynamics on multiplex networks

Xin Chang,[1,2,3] Chao-Ran Cai,[1,3,*] Chong-Yang Wang,[4] Xu-Sheng Liu,[5] Ji-Qiang Zhang,[6] Kang Jin,[1] and Wen-Li Yang[2,3]

[1]*School of Physics, Northwest University, Xi'an 710127, China*

[2]*Institute of Modern Physics, Northwest University, Xi'an 710127, China*

[3]*Shaanxi Key Laboratory for Theoretical Physics Frontiers, Xi'an 710127, China*

[4]*Yangtze Delta Region Institute of University of Electronic Science and Technology of China, Huzhou, Zhejiang, 313000, China*

[5]*School of Science, East China University of Technology, Nanchang, Jiangxi 330013, China*

[6]*School of Physics and Electronic-Electrical Engineering, Ningxia University, Yinchuan 750021, China*

(Received 29 June 2022; accepted 20 February 2023; published 21 March 2023)

In this paper, we investigate the effect of self-awareness (interlayer interaction) for information-epidemic dynamics with simplicial complexes both near and away from the epidemic threshold. It is shown that, contrary to previous views, self-awareness plays a key role near the epidemic threshold. In small homogeneous networks, multiple susceptibility peaks can emerge in the susceptibility of the epidemic layer under the combined effect of simplicial complexes and self-awareness, even two types of multiple susceptibility peaks with completely opposite mechanisms. This means that one needs to be very careful when obtaining epidemic thresholds based on susceptibility. Moreover, the self-awareness can regulate the presence or absence of bistable phenomena both in epidemic prevalence and epidemic threshold. We also found that the time series of disease may be nonmonotonic, with a peak, and that self-awareness is one of the factors controlling the relative height between maximum and steady state. In addition, we modify heterogeneous mean-field theory and partial effective degree theory to accommodate the introduction of simplicial complexes in dynamics. We believe that our study has implications for other dynamics concerning higher-order and interlayer interactions.

DOI: 10.1103/PhysRevResearch.5.013196

I. INTRODUCTION

As a disease spreads through a population, information about the disease will be diffused and individual behavior will change with the diffusion [1]. Mutual feedback emerges between information diffusion process and epidemic spreading process [2,3]: individuals may know information about the disease through their own illness (called self-awareness), and individuals who know the information may change their behavior to protect themselves and others. In earlier studies, Funk *et al.* [4,5] and Kiss *et al.* [6] have independently built theoretical models incorporating these two spreading processes in a well-mixed population. Subsequently, many researchers began to study human responses to outbreaks in network epidemic models [7–9]. Considering the diversity and complexity of information diffusion [10,11], more rational multiplex networks [12–16] have been used to explore the interaction between epidemic spreading and information diffusion [17–29]. In previous studies, the probability of self-awareness was usually set at one [25–27] or some other fixed values [20,24], because this probability did not affect the epidemic threshold [18,19]. This characteristic of self-awareness is caused by the fact that information diffusion is thought of as a "simple contagions," a simple superposition of pairwise interaction, similar to epidemic spreading [30,31].

However, information diffusion usually requires contact with multiple sources of "infection" [32–34], which is called social reinforcement [33,35] or "complex contagions" [32,36]. Here, the exposure to multiple sources of infection is different from that of multiple exposures to a single source [37,38]. A natural explanation for complex contagions is that multiple simultaneous interactions (or group interactions) give rise to an additional probability of infection, which can be described in terms of higher-order interactions [39–44], including simplicial complexes [45–48] and hypergraphs [49–51]. Recently, the research enthusiasm for higher-order interactions has swept through many fields, such as network epidemiology [52–56], network synchronization [57], brain network [58], and ecological system [59]. The study of high-order interactions is conducive to better understand, analyze and predict dynamic behaviors on complex networks, and may also lead to new research problems and objects.

As mentioned above, the additional ability of social groups to transmit information can be described by simplicial complexes. In general, group interactions require a certain proportion of aware individuals in a system to function, so the dynamic on simplicial complexes often depend on the initial seeds to determine evolutionary stable states [53–56], such as discontinuous transitions and bistable phenomena. For a

*ccr@nwu.edu.cn

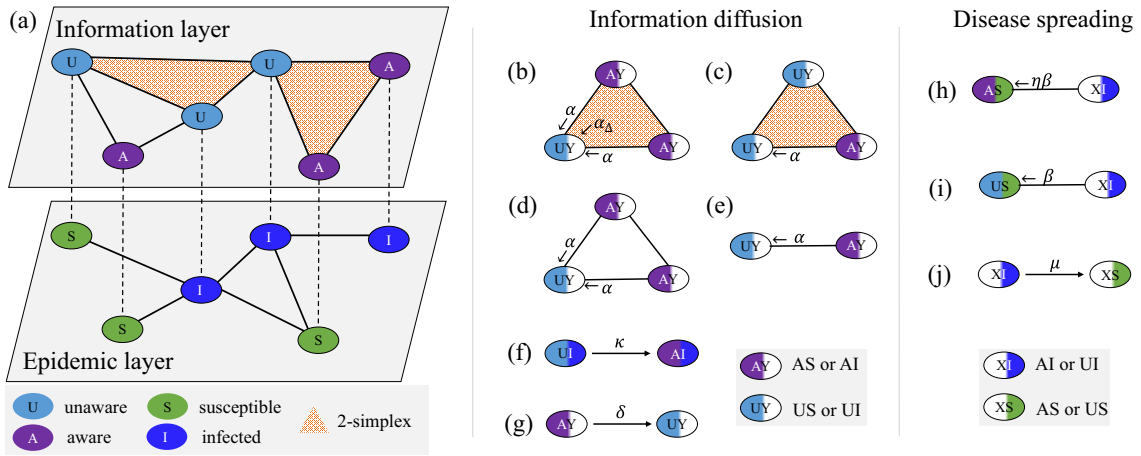

FIG. 1. (a) Schematic illustration of UAU-SIS model on a multiplex network with simplicial complexes. The upper layer corresponds to the network where the information of epidemic diffuses. Nodes can be either aware (A) or unaware (U), and interations include pairwise interations and 2-simplices which represent by links and checked pattern areas, respectively. The lower layer represents the network where the epidemic spreads. Nodes have two possible states—infected (I) and susceptible (S), and interactions are only pairwise interactions between adjacent nodes. There are four classes of states on the multiple networks: unaware and susceptible (US), unaware and infected (UI), aware and susceptible (AS), and aware and infected (AI). Here, XI ∈ {AI, UI}, XS ∈ {AS, US}, AY ∈ {AS, AI}, and UY ∈ {US, UI}. [(b)–(j)] Schematic representations of the transitions between node states and their associated probabilities. [(b)–(e)] An unaware node is informed by an aware neighbor with probability α through links. An unaware node can receive the information with extra probability α_Δ if the two other nodes in the 2-simplex are aware in panel (b). Note that there is no extra probability α_Δ if a triangle is "empty" as in panel (d) or less than two aware individuals as in panel (c). (f) UI nodes become AI due to self-awareness with probability κ. (g) An aware individual forgets information with probability δ. A susceptible node is infected by an infectious neighbor with probability $\eta\beta$ in panel (h) or β in panel (i) when the susceptible node is aware or unaware, respectively. (j) Infected nodes recover with probability μ.

multiplex network, the interlayer interaction (e.g., self-awareness of information-epidemic dynamics) brings in external inputs between layers of the network, which can act as initial seeds. Here, we introduce simplicial complexes into the classical coupled information-epidemic dynamics model (that is, UAU-SIS model). We find that the presence or absence of bistable phenomena is regulated by self-awareness, both in terms of epidemic prevalence and epidemic threshold. Under the combined effect of simplicial complexes and self-awareness, the susceptibility of epidemic layer presents two kinds of bimodal curves with completely different physical mechanisms, which means that the judgment of threshold value should be very careful. Meanwhile, it is found that the time series of diseases may show a peak, which seems to be unusual in SIS model.

Our paper is organized as follows. In Sec. II, we describe the UAU-SIS model with simplicial complexes in detail and give the procedures for generating multiplex networks. In Sec. III, we develop a modified heterogeneous mean-field theory to analyze the dynamics of the single information layer. In Secs. IV and V, we discuss the cases near and far from the epidemic threshold for UAU-SIS model on multiplex networks, respectively. The bistable region in Sec. III is the main parameter range studied. In Sec. VI, we summarize our results.

II. MODEL

A. Discrete-time UAU-SIS model with simplicial complexes

Simplicial complexes are to treat social groups as simplexes, and a simplex defines a k-simplex as a set of $k+1$ nodes [53]. For example, 0-simplices and 1-simplices correspond to nodes and links, which have been considered in "simple contagions"; 2-simplices correspond to "full" triangles; 3-simplices correspond to "full" tetrahedra. A k-simplex down contains all the subfaces, for example, a 2-simplex has three 1-simplices and three 0-simplices. In this paper, we introduce 2-simplices into the information layer of the classical UAU-SIS model, which is embedded in a two-layer multiplex network making up an epidemic layer and an information layer. The discrete-time UAU-SIS model with simplicial complexes is shown in Fig. 1(a). In the information layer, if one individual is aware of epidemic information, then its state is aware (A), otherwise its state is unaware (U). In the epidemic layer, individuals are either in the infected (I) state or susceptible (S) state. Therefore, individuals in the multiplex network can be divided into four different classes: unaware and susceptible (US), unaware and infected (UI), aware and susceptible (AS), and aware and infected (AI).

In the information layer, the interactions includes pairwise interaction between adjacent nodes (1-simplices) and group interaction (2-simplices), and the schematic illustration of the state transitions is shown in Figs. 1(b)–1(g). For the pairwise interaction, an unaware node is informed with probability α from an aware neighbor, see Figs. 1(b)–1(e). For the group interaction, an unaware node can also be informed with probability α_Δ if the rest nodes in the 2-simplex are aware, see Fig. 1(b). Note that an "empty" triangle is not a 2-simplex, see Fig. 1(d). Meanwhile, as a result of self-awareness, UI nodes can become to AI with probability κ; see Fig. 1(f). Therefore, the probabilities that from US to AS and from UI to AI are $1-(1-\alpha)^{n_a}(1-\alpha_\Delta)^{n_\Delta}$ and $1-(1-\kappa)(1-$

TABLE I. Parameters found in discrete-time UAU-SIS model with simplicial complexes.

Parameter	Description
α	Transmission probability of an unaware node interacting with an aware neighbor
α_Δ	Transmission probability of an unaware node interacting with a group containing a"full" triangle and two other aware nodes
κ	Self-awareness probability of an unaware node when it is infected
δ	Recovery probability for an aware node
β	Transmission probability of an susceptible node interacting with an infected neighbor
μ	Recovery probability for an infected node
η	Strength of protective measures taken byaware nodes

$\alpha)^{n_a}(1-\alpha_\Delta)^{n_\Delta}$, respectively, where n_a is the number of aware neighbors of the unaware individual and n_Δ represents the number of 2-simplices satisfying Fig. 1(b). An aware individual forgets information with probability δ, see Fig. 1(g).

Figures 1(h)–1(j) are the schematic representations of the state transitions in the epidemic layer. Susceptible individuals in the US class and AS class are infected by one of its infected neighbors with probabilities β and $\eta\beta$, respectively. The parameter $\eta \in [0, 1]$ represents the strength of protective measures taken by aware individuals. Then, the probabilities that from US to UI and from AS to AI are $1-(1-\beta)^{n_i}$ and $1-(1-\eta\beta)^{n_i}$, respectively, where n_i denotes the number of infected immediate neighbors of the susceptible individual. An infected individual recovers to be susceptible with probability μ, regardless of whether it is aware or unaware. Table I presents a complete list and description of all parameters in the model.

B. Generation of multiplex networks with simplicial complexes

In a multiplex network, the network topology of each layer is usually different, which means the neighbors for any node maybe different in the two layers.

For the information layer, we employ the random simplicial complex (RSC) model used in Refs. [47,53]. The RSC model can control and tune the average degree $\langle k_1\rangle$ and the expected number of 2-simplices $\langle k_\Delta\rangle$, and the generation process is as follows:

Step 1: Create an Erdős-Rényi (ER) network [60] by connecting any pair of nodes with probability $p_1 = \frac{\langle k_1\rangle - 2\langle k_\Delta\rangle}{(N-1)-2\langle k_\Delta\rangle}$, where N is network size. Note that the "empty" triangle produced by this step is not a 2-simplex.

Step 2: 2-simplexes are created by connecting any triplet of vertices (avoiding multiple edges) with probability $p_2 = \frac{2\langle k_\Delta\rangle}{(N-1)(N-2)}$.

The joint distribution of degree and 2-simplices degree (which is the number of 2-simplices incident on the node) $P_1(k_1, k_\Delta)$ on the information layer can be written as

$$P_1(k_1, k_\Delta) = P'(k_1 - 2k_\Delta)P''(k_\Delta), \tag{1}$$

where $P'(k_1)$ and $P''(k_\Delta)$ are the distribution of degree only from step 1 and the distribution of 2-simplices degree from step 2, respectively. And they can be obtained from the following formulas:

$$P'(k_1) = \binom{N-1}{k_1}(1-p_1)^{N-1-k_1}p_1^{k_1},$$
$$P''(k_\Delta) = \binom{\binom{N-1}{2}}{k_\Delta}(1-p_2)^{\binom{N-1}{2}-k_\Delta}p_2^{k_\Delta}.$$

Then, the degree distribution of the information layer can be calculated as

$$P_1(k_1) = \sum_{k_\Delta} P_1(k_1, k_\Delta). \tag{2}$$

For the epidemic layer, we use Poisson distribution $P_2(k_2) \approx e^{-\langle k_2\rangle}\langle k_2\rangle^{k_2}/k_2!$, where $\langle k_2\rangle$ is the average degree of an ER random network. Considering that we live in the era of information, we fix $\langle k_1\rangle = 20$, $\langle k_\Delta\rangle = 6$, $\langle k_2\rangle = 6$, and $N = 2000$ in the paper.

III. MODIFIED HETEROGENEOUS MEAN-FIELD THEORY ON SINGLE UAU LAYER

The original heterogeneous mean-field theory [61] proposed for the SIS model on a single-layer network focuses on the probability that individuals with same degree are in a compartment, which can not capture the effect of simplicial complexes. Here, we propose a modified heterogeneous mean-field theory by introducing the number of 2-simplices of each individual, k_Δ, as an additional trace. For example, A_{k_1,k_Δ} (U_{k_1,k_Δ}) denotes the relative density of aware (unaware) individuals with degree k_1 and 2-simplices degree k_Δ.

We denote ϕ as the probability that an aware individual is in contact with any unaware individual, that is, $\phi = \frac{1}{\langle k_1\rangle}\sum_{k_1}\sum_{k_\Delta} k_1 P_1(k_1, k_\Delta)A_{k_1,k_\Delta}$, which is independent of degree k and 2-simplices degree k_Δ. For an unaware individual with given k_1 and k_Δ, the probabilities that it is not infected by any pairwise interaction and any 2-simplex are $(1-\alpha\phi)^{k_1}$ and $(1-\alpha_\Delta\phi^2)^{k_\Delta}$, respectively. Then, the Markov-chain equations of the modified heterogeneous mean-field theory are as follows:

$$A_{k_1,k_\Delta}(t+1) = -[1-\alpha\phi(t)]^{k_1}[1-\alpha_\Delta\phi(t)^2]^{k_\Delta}U_{k_1,k_\Delta}(t) - \delta A_{k_1,k_\Delta}(t) + 1, \tag{3}$$

where $A_{k_1,k_\Delta}(t) + U_{k_1,k_\Delta}(t) = 1$. When the population reaches its steady state, i.e., $A_{k_1,k_\Delta}(t+1) = A_{k_1,k_\Delta}(t) = A_{k_1,k_\Delta}$, Eq. (3) becomes

$$A_{k_1,k_\Delta} = \frac{1-(1-\alpha\phi)^{k_1}(1-\alpha_\Delta\phi^2)^{k_\Delta}}{\delta + 1 - (1-\alpha\phi)^{k_1}(1-\alpha_\Delta\phi^2)^{k_\Delta}}. \tag{4}$$

After substituting Eq. (4) into ϕ, we can obtain a self-consistent equation for ϕ,

$$\frac{1}{\langle k_1\rangle}\sum_{k_1,k_\Delta}\frac{k_1 P_1(k_1,k_\Delta)[1-(1-\alpha\phi)^{k_1}(1-\alpha_\Delta\phi^2)^{k_\Delta}]}{\delta + 1 - (1-\alpha\phi)^{k_1}(1-\alpha_\Delta\phi^2)^{k_\Delta}} = \phi. \tag{5}$$

Combining Eqs. (4) and (5), we can obtain A_{k_1,k_Δ} in the steady state. And then, the fraction of aware individuals is calculated

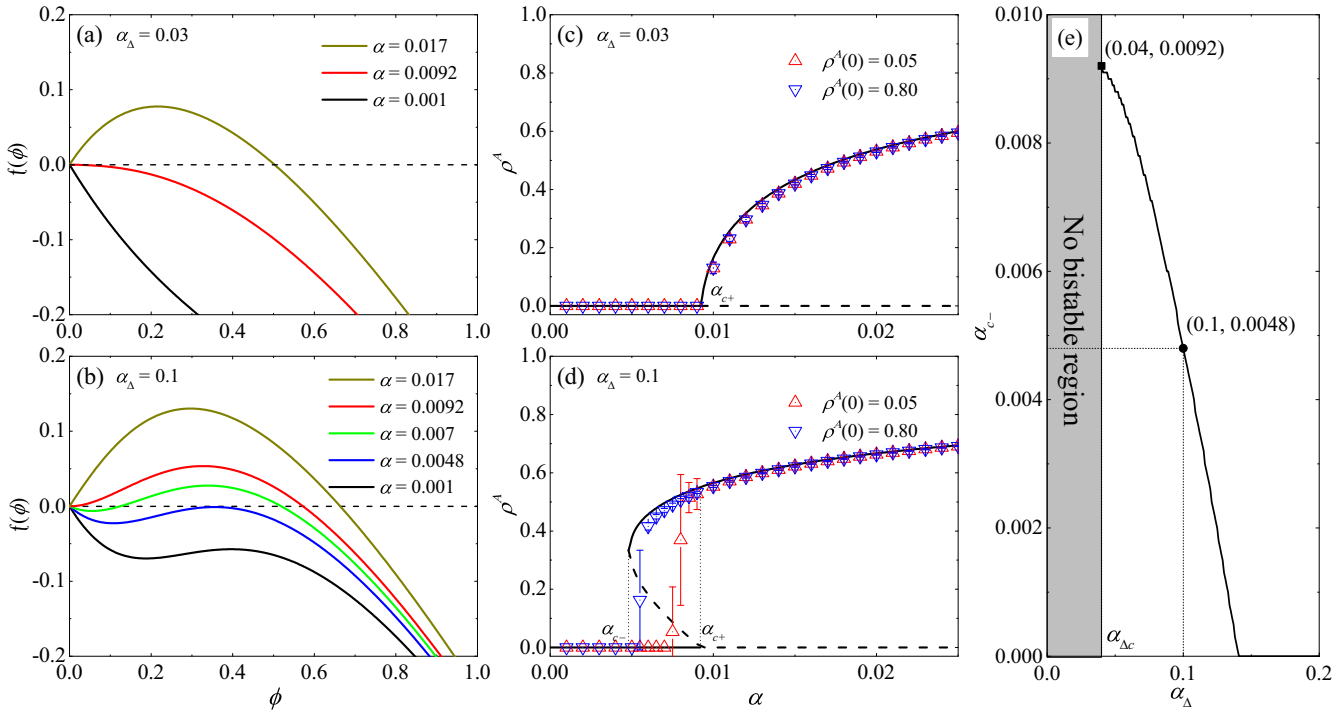

FIG. 2. (a),(b) $f(\phi)$ as a function of ϕ for different α and α_Δ on RSC model. (c)-(d) The fraction of aware individuals ρ^A as a function of the awareness probability α on RSC model. (e) The relation between α_{c-} and α_Δ from Eq. (9). Parameters: $N = 2000$, $\langle k_1\rangle = 20$, $\langle k_\Delta\rangle = 6$, and $\delta = 0.2$. When $\alpha = 0.0092$, the curve $f(\phi)$ is tangent to the horizontal axis at $\phi = 0$ both in panels (a),(b). When $\alpha = 0.0048$, the curve $f(\phi)$ is tangent to the horizontal axis at $\phi \neq 0$ in panel (b). In panels (c),(d), the lines are theoretical results from Eqs. (4)–(6) where the stable solutions are represented by solid lines and unstable solutions by dashed lines, and the scatters are the results from stochastic simulations which are averaged over 100 independent runs.

by

$$\rho^A = \sum_{k_1,k_\Delta} P_1(k_1,k_\Delta)A_{k_1,k_\Delta}. \tag{6}$$

Since the fraction of aware individuals is increasing with ϕ monotonically, the qualitative property of ρ^A is identical to that of ϕ. Here, we define the left-hand side of Eq. (5) minus its right-hand side as $f(\phi)$, that is,

$$f(\phi) = \sum_{k_1,k_\Delta} \frac{k_1 P_1(k_1,k_\Delta)[1-(1-\alpha\phi)^{k_1}(1-\alpha_\Delta\phi^2)^{k_\Delta}]}{\langle k_1\rangle[\delta+1-(1-\alpha\phi)^{k_1}(1-\alpha_\Delta\phi^2)^{k_\Delta}]} - \phi. \tag{7}$$

For different strength of higher-order efferts α_Δ, $f(\phi)$ shows different dynamical behaviors. There is a critical value, $\alpha_{\Delta c}$, that distinguishes Fig. 2(a) from Fig. 2(b), whose value can be approximated by $\delta/\langle k_\Delta\rangle$ obtained from the mean-field theory for homogeneous networks in Ref. [53]. For $\alpha_\Delta < \alpha_{\Delta c}$, a saddle node bifurcation emerges in $f(\phi)$ with the increase of α in Fig. 2(a), while the bifurcation turns into a supercritical fork bifurcation for $\alpha_\Delta > \alpha_{\Delta c}$; see Fig. 2(b). From the fact that α_{c-} is less than α_{c+} (they are defined later), it is possible to solve numerically for an exact $\alpha_{\Delta c}$; see Fig. 2(e). The value of $\alpha_{\Delta c}$ depends not only on the dynamical parameters but also on the specific network structure.

Figure 2 shows that there are three cases for different α and α_Δ. For the parameters with one solution at $\phi = 0$, i.e., the black and red lines with $\alpha = 0.001$ and $\alpha = 0.0092$ in Figs. 2(a) and 2(b), it is obviously that ρ^A is also zero, which indicates a disease free state. For the parameters with two solutions, i.e., the dark yellow lines with $\alpha = 0.017$ in Figs. 2(a) and 2(b), the stability analysis shows the high one is stable, which indicate that global outbreaks are inevitable. For the above two cases, ρ^A is independent of the initial conditions [i.e., $\rho^A(0)$]; see Figs. 2(c) and 2(d). The red lines with $\alpha = 0.0092$ in Figs. 2(a) and 2(b), which are tangent to the horizontal axis at $\phi = 0$, are the critical point for the above global outbreaks, whose corresponding α_{c+} can be obtained by $\frac{df(\phi)}{d\phi}|_{\phi=0} = 0$, so that we have

$$\alpha_{c+} = \delta\frac{\langle k_1\rangle}{\langle k_1^2\rangle}, \tag{8}$$

where $\langle k_1^2\rangle$ is the second moment of degree k_1.

For the parameters with three solutions, i.e., the green line with $\alpha = 0.007$ in Fig. 2(b), the stability analysis shows the middle fixed point is unstable and the others are stable as in the supercritical fork bifurcation. In this case, ρ^A depends on the initial conditions and a hysteresis loop can be observed; see Fig. 2(d). The blue line with $\alpha = 0.0048$ in Fig. 2(b) is tangent to the horizontal axis at $\phi \neq 0$, which is the critical point of one solution and three solutions. The corresponding α_{c-} can be obtained from

$$\begin{aligned} \left.\frac{df(\phi)}{d\phi}\right|_{\phi\neq 0} &= 0, \\ f(\phi)|_{\phi\neq 0} &= 0. \end{aligned} \tag{9}$$

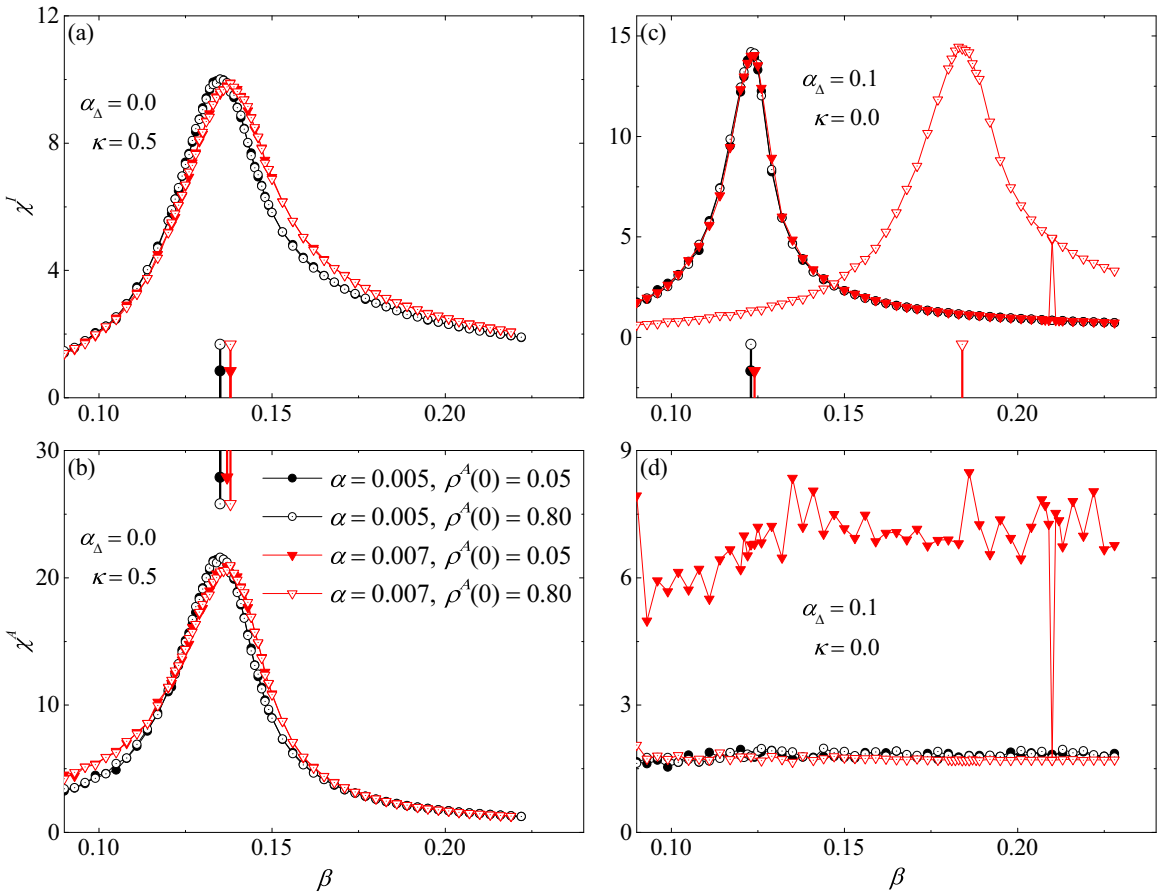

FIG. 3. The susceptibilities χ^I and χ^A as function of infection probability β without 2-simplices in panels (a),(b) or without self-awareness in panels (c),(d). The peaks of the curves have been specially marked for clearer comparison. The information layer uses a RSC network with $\langle k_1 \rangle = 20$ and $\langle k_\Delta \rangle = 6$, and the epidemic layer is an ER network with $\langle k_2 \rangle = 6$. Parameters: $N = 2000$, $\delta = 0.2$, $\eta = 0.3$, $\mu = 0.8$.

The numerical relation between α_{c-} and α_Δ is shown in Fig. 2(e), and α_{c-} is equal to zero when α_Δ is greater than 0.140.

From Figs. 2(c) and 2(d), one learns that the results from the modified heterogeneous mean-field theory match quite well with those obtained from Monte Carlo simulations on a random simplicial complex network.

IV. EPIDEMIC THRESHOLD OF MULTIPLEX NETWORKS

In previous studies on information-disease dynamics on multiplex networks [17,18,24], the information layer was assumed to be updated before the disease layer within a same time step. This assumption is based on the perception that information spreads faster than disease, which is reasonable in most cases. But the small awareness probability α does not seem to meet the assumption, especially in our focus bistable region in information layer [see Fig. 2(d)]. Here, we assume that both the disease layer and the information layer are updated only depending on the state of the last time step, and we show in the Appendix A that the update order of UAU-SIS model on multiplex networks is actually trivial.

Generally speaking, the order parameter fluctuates greatly near the phase transition point. Here, we employ the the quasistationary (QS) simulation method [62] to analyze the fluctuation of the UAU-SIS system. The procedure is implemented as follows: First, a list of M active configurations is established to store states previously visited by the dynamics. Whenever the system tries to enter the absorbing state ($\rho^I = 0$ or/and $\rho^A = 0$), it jumps to an active configuration selected from the list randomly. And the list is updated constantly in a way that a randomly selected configuration is replaced by the present active configuration with a probability $p_r \Delta t$. Next, after a long relaxation time t_r, we capture samples of the number of infected and aware individuals at each time step during a period of time t_a. The probabilities $P_{\rm A}(m)$ and $P_{\rm I}(n)$ that the system has m aware individuals and has n infected individuals can be counted by samples, respectively. Then, the moments of the activity distribution can be computed as $\langle (\rho^A)^k \rangle = \sum_m (m/N)^k P_{\rm A}(m)$ and $\langle (\rho^I)^k \rangle = \sum_n (n/N)^k P_{\rm I}(n)$. Finally, the susceptibilities χ^I and χ^A can be obtained by $\chi^I = N(\langle (\rho^I)^2 \rangle - \langle \rho^I \rangle^2)/\langle \rho^I \rangle$ and $\chi^A = N(\langle (\rho^A)^2 \rangle - \langle \rho^A \rangle^2)/\langle \rho^A \rangle$. The values of the QS parameters used in Figs. 3–6 are $M = 100$, $p_r = 0.05$, $t_r = 2 \times 10^6$, and $t_a = 3 \times 10^6$ (near the first peak of the bimodal curve in Fig. 3, we use $t_r = 5 \times 10^7$ and $t_a = 5 \times 10^6$ to ensure that the curve is smooth).

A. Analysis of multiple susceptibility peaks

Figure 3 plots the susceptibilities χ^I and χ^A as function of infection probability β without 2-simplices

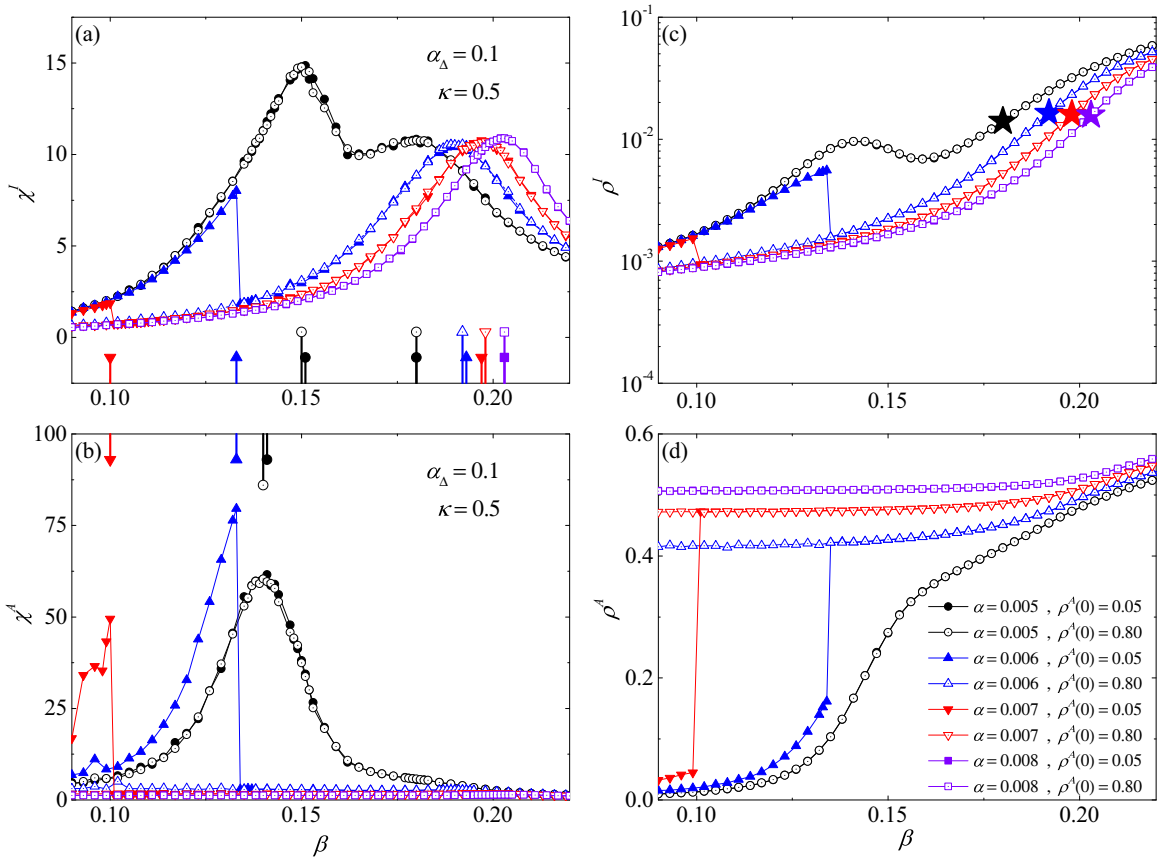

FIG. 4. (a),(b) The susceptibilities χ^I and χ^A as function of infection probability β in the presence of both 2-simplices and self-awareness. (c),(d) The fractions of infected individuals and aware individuals as function of infection probability β. The peaks of the curves have been specially marked for clearer comparison in panels (a),(b). The star symbol in panel (c) marks the critical masses of the finite system corresponding to these epidemic thresholds. The information layer uses a RSC network with $\langle k_1 \rangle = 20$ and $\langle k_\Delta \rangle = 6$, and the epidemic layer is an ER network with $\langle k_2 \rangle = 6$. Parameters: $N = 2000$, $\delta = 0.2$, $\eta = 0.3$, $\mu = 0.8$.

($\alpha_\Delta = 0$) or self-awareness ($\kappa = 0$). Figure 4 plots the susceptibilities and average propagation sizes as function of infection probability β in the presence of both 2-simplices and self-awareness. Here, the selection of parameters $\alpha_\Delta = 0.1$ and $\alpha \in [0.005, 0.008]$ limits to the bistable region in Fig. 2.

When self-awareness probability is high but without 2-simplices, i.e., Figs. 3(a) and 3(b), the peak values of χ^I are consistent with those of χ^A under the same parameters and the results are not affected by the initial seeds $\rho^A(0)$. In this case, the information layer cannot propagate information through either pairwise interactions or 2-simplices. The fluctuation of ρ^A is related to that of ρ^I through the feedback of self-awareness κ. When there is 2-simplices in the system but no self-awareness, i.e., Figs. 3(c) and 3(d), the information layer is independent of the epidemic layer. With the feedback through aware individuals taking protective measures, the fluctuation of ρ^I on the epidemic layer can produce the bistabling with the dependence of the initial seeds $\rho^A(0)$, such as $\alpha = 0.007$ in Fig. 3(c).

For the case of $\alpha_\Delta = 0.1$ and $\kappa = 0.5$, it shows a variety of phenomena for the slow growth of α in Figs. 4(a) and 4(b). For $\alpha = 0.005$ in Fig. 4(b), the fluctuation of the information layer comes from whether a large number of 2-simplices are activated in the information layer itself, and self-awareness feedback depending on whether the epidemic layer breaks out. And there is a mechanism of mutual restriction between them. The increase of β not only promotes the spread of the disease, but also increases the number of aware individuals through self-awareness as well. The latter promotes the spread on information layer by 2-simplices, and as a result, the aware individuals generated by 2-simplices in turn suppress the spread of the disease. This mutual conditioning mechanism allows the fraction of aware individuals to increase smoothly, see $\alpha = 0.005$ of Fig. 4(d). However, when the activation point of 2-simplices is far below the epidemic threshold, the above competition can be ignored. As a result, there is a sudden increase in the informant layer when $\alpha = 0.006, 0.007$ and $\rho^A(0) = 0.05$ in Fig. 4(d), which depends on group interactions generating a cascade of activations. Thus, it shows a sharp and discontinuous drop of χ^A in Fig. 4(b). Meanwhile, we know that whether a number of 2-simplices are activated depends on the fraction of aware individuals in the population which is proportional to α, β, and κ, so Fig. 4(b) shows that the peak location of χ^A moves to the left as α increases.

The fluctuation of epidemic layer depends on whether the epidemic layer breaks out or not and on the fluctuation of aware individuals, the latter depends on whether the 2-simplices of the information layer are activated. Compared with Figs. 4(a) and 4(b), we find that χ^I reaches its peak not earlier than the peak of χ^A with the increase of β, because

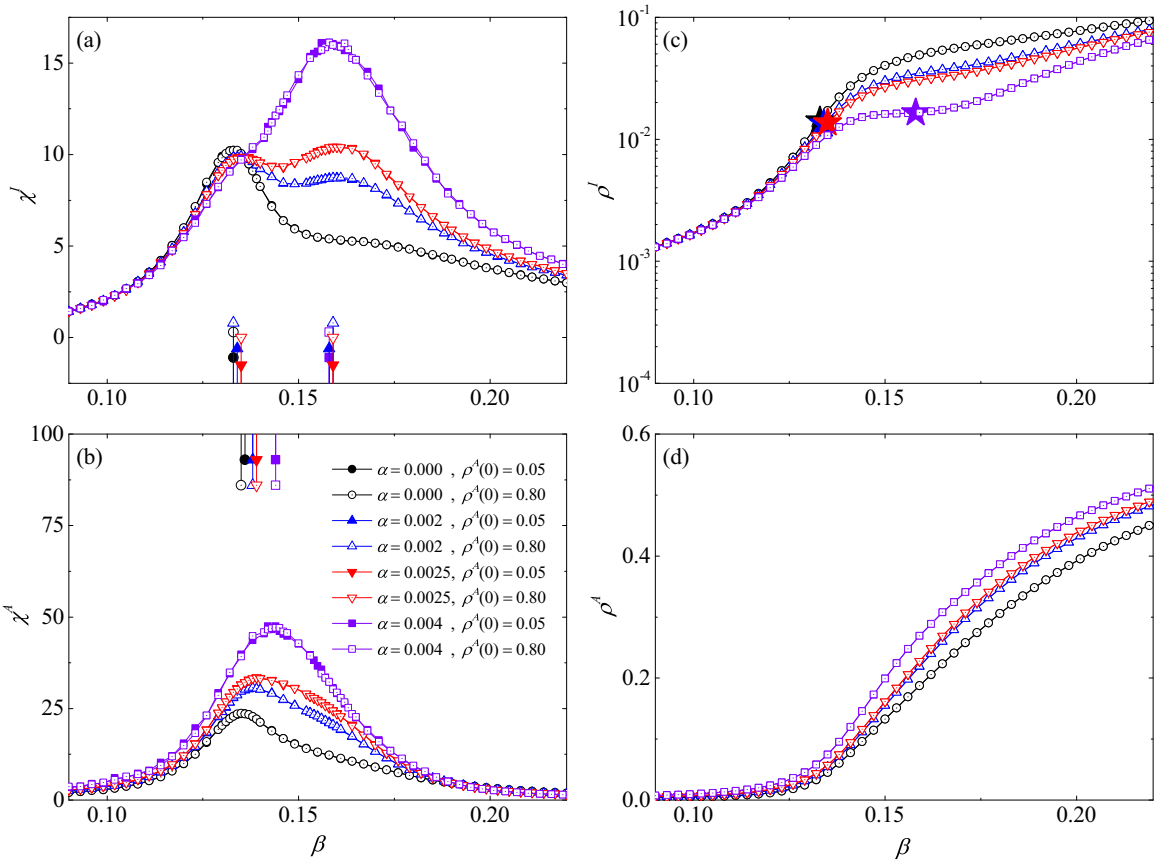

FIG. 5. (a),(b) The susceptibility χ^I and χ^A as a function of infection probability β for low α. (c),(d) The fractions of infected individuals and aware individuals as function of infection probability β. The peaks of the curves have been specially marked for clearer comparison in panels (a),(b). The star symbol in panel (c) marks the critical masses of the finite system corresponding to these epidemic thresholds. The information layer uses a RSC network with $\langle k_1 \rangle = 20$ and $\langle k_\Delta \rangle = 6$, and the epidemic layer is an ER network with $\langle k_2 \rangle = 6$. Parameters: $N = 2000$, $\delta = 0.2$, $\eta = 0.3$, $\mu = 0.8$, $\alpha_\Delta = 0.1$, $\kappa = 0.5$.

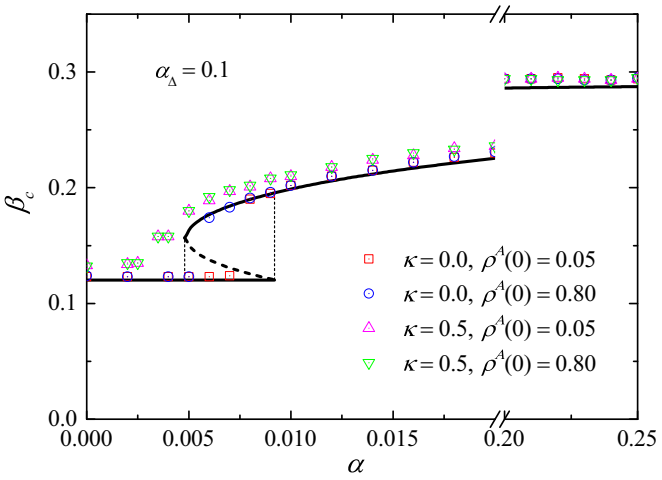

FIG. 6. The epidemic threshold β_c as a function of awareness probability α. The information layer uses a RSC network with $\langle k_1 \rangle = 20$ and $\langle k_\Delta \rangle = 6$, and the epidemic layer is an ER network with $\langle k_2 \rangle = 6$. Line is the theoretical estimations of Eq. (10), while scatters are simulation results obtained by the peaks of χ^I (the peak of the unimodal curve or the second peak of the bimodal curve). The other parameters: $N = 2000$, $\delta = 0.2$, $\eta = 0.3$, $\mu = 0.8$, $\alpha_\Delta = 0.1$.

the activation of 2-simplices produces a number of aware individuals, which suppress the spread of the disease. With the increase of α, the epidemic threshold gradually increases while the activation point of 2-simplices gradually decreases. The first peak is dominated by activation of 2-simplices. To be specific, the cascade of activation of group interactions leads to a decrease in the average infection rate of the epidemic layer, and we can see a sudden decrease in the fraction of infected individuals in Fig. 4(c), which drives a large fluctuation in the epidemic layer. The epidemic threshold is the phase transition point from disease-free state to endemic state in the thermodynamic limit. Although a finite-size system will have a certain propagation size at its epidemic threshold, this size cannot show a downward trend. Therefore, we conclude that the epidemic threshold is the β corresponding to the second peak rather than the first peak in the epidemic layer. In addition, it can be seen from Fig. 4(c) that the critical masses around these threshold points of the disease spreading are not much different. From Fig. 4(a), we can see that the initial seeds $\rho^A(0)$ can affect the first peak but not affect the epidemic threshold.

The epidemic threshold (the second peak) fluctuates randomly by 0.001, while the first peak fluctuates by about 0.005.

B. Another kind of multiple susceptibility peaks

In Fig. 5, we test the susceptibility χ^I and χ^A when α is lower than 0.005. Figure 5(a) also shows a bimodal curve, but its physical mechanism is completely different from that in Fig. 4(a). It is clear to see that the peak of χ^A appears later than the first peak of χ^I for $\alpha \in [0, 0.0025]$ with the increase of β, which indicates that the epidemic layer breaks out before χ^A reaches its peak. At this point, the activation of 2-simplices depends mainly on the large number of aware individuals brought by the outbreak of epidemic layer. Because of the mutual constraint mechanism mentioned earlier, we can see that Fig. 5(d) is all smooth curves. In these bimodal curves, the first peak and the second peak are dominated by the epidemic threshold and the activation of 2-simplices, respectively, which is exactly opposite to Fig. 4(a). In addition, the critical masses around these threshold points in Fig. 5(c) and Fig. 4(c) does not differ much.

Meanwhile, Figure 5(b) shows that the peak location of χ^A moves to the right as α increases, which is also contrary of Fig. 4(b). Generally, the increase of α suppresses the spread of the disease. Although we can see in Fig. 5(a) that a low α has little effect on the epidemic threshold, it still reduces the infected individuals when β is greater than the threshold which can refer to the slope change in Fig. 5(b). According to the feedback of self-awareness, the increase of α indirectly slows down the accumulation of external input aware individuals, so the peak location of χ^A moves to the right.

C. Epidemic threshold

In Fig. 6, we plot the epidemic threshold β_c as a function of awareness probability α for $\alpha_\Delta = 0.1$. The simulation results of the epidemic threshold β_c are obtained from the peaks of curves χ^I. According to the Sec. IV A and Sec. IV B, β_c can be obtained from the following three cases: (i) the peak location of single-peak curve; (ii) the first peak's location of the bimodal curve when the first peak of χ^I appears earlier than the peak of χ^A; (iii) the second peak's location of the bimodal curve when the first peak of χ^I appears not earlier than the peak of χ^A.

Without self-awareness in Fig. 6, the epidemic threshold reveals an abrupt transition and the critical point at which the transition occurs is related to the initial seeds $\rho^A(0)$. However, for $\kappa = 0.5$, the epidemic threshold is independent of $\rho^A(0)$, because the self-awareness of infected individuals provides a number of aware individuals to ensure the activation of 2-simplices. Moreover, it is easy to see in Fig. 6 that the threshold of $\kappa = 0.5$ is larger than that of $\kappa = 0$ for low α, while the above two thresholds are coincident for high α. The reason is that the number of aware individuals generated by self-awareness can be ignored when α is high.

To obtain an analytical epidemic threshold, we approximate the information layer as an annealed network (all the nodes are same in this layer) and ignore the aware individuals obtained from self-awareness (i.e., $\kappa = 0$). Since the information layer is in thermodynamic dynamic equilibrium, the average infected probability in epidemic layer is approximately $\rho^U + \eta\rho^A$ [24]. Then, the epidemic threshold β_c can be calculated as

$$\beta_c = \frac{\beta_c^{\text{single}}}{1 - (1-\eta)\rho^A}, \tag{10}$$

where β_c^{single} denotes the epidemic threshold of the single SIS layer which is decoupled from the multiplex network, and ρ^A indicates the fraction of aware individuals of the single UAU layer which is decoupled from the multiplex network. The stationary solutions of ρ^A can be calculated by the modified heterogeneous mean field theory, i.e., Eqs. (4)–(6) in Sec. III. β_c^{single} in Eq. (10) can be calculated by many theoretical approaches, such as microscopic Markov-chain approach [63], epidemic link equations approach [64], and effective degree Markov-chain approach [65]. In Fig. 6, we use dynamic correlation method [66] to calculate β_c^{single}, which considers the dynamic correlation of immediate neighbors and ignores the higher-order neighbors. The relation is as follows

$$\langle k_2\rangle\left(1-\beta_c^{\text{single}}\right)(1-\mu) + \langle k_2(k_2-1)\rangle\beta_c^{\text{single}} = \left\langle k_2\left[1-\beta_c^{\text{single}} + \beta_c^{\text{single}}\mu + \left(1-\beta_c^{\text{single}}-\mu\right)\mu\frac{\langle k_2\rangle}{\langle k_2^2\rangle}\right]^{k_2}\right\rangle. \tag{11}$$

V. RESULTS FAR FROM THE THRESHOLD

A. Epidemic prevalence

In what follows we investigate how the group interaction in 2-complex affect the epidemic prevalence in the UAU-SIS model. In Fig. 7, we plot the epidemic prevalence ρ^I as a function of α_Δ for different awareness probabilities α and initial seeds $\rho^A(0)$. When $\alpha_\Delta < \alpha_{\Delta c}$ or $\alpha < \alpha_{c-}$, i.e., the shaded area of Fig. 7(a), the information layer cannot affect the epidemic layer because the information cannot spread out. For the unshaded area of Fig. 7(a), which satisfies $\alpha_\Delta > \alpha_{\Delta c}$ and $\alpha \in (\alpha_{c-}, \alpha_{c+})$, the epidemic prevalence may be suppressed by increasing α_Δ, but there is a certain failure rate, which is related to the initial seeds on the information layer. Namely, the more initial seeds there are in the information layer, the more effective and stable it is to suppress the epidemic prevalence. Notice that α_{c+} can be obtained by Eq. (8) and α_{c-} can be expressed as a function of α_Δ. For $\alpha > \alpha_{c+}$ in Fig. 7(b), the results of prevalence are independent of the initial seeds.

From Fig. 7(b), one learns that the increase of α_Δ can effectively inhibit the disease only when α is low. With the increase of α, such as $\alpha = 0.1$ and 0.5, the inhibitory effect of α_Δ on disease decreases significantly. For low α, the pairwise interaction cannot effectively spread information, resulting in a large number of unaware individuals in the network when the 2-simplices is missing. But the fraction of unaware nodes in the population is already very small for high α (less than

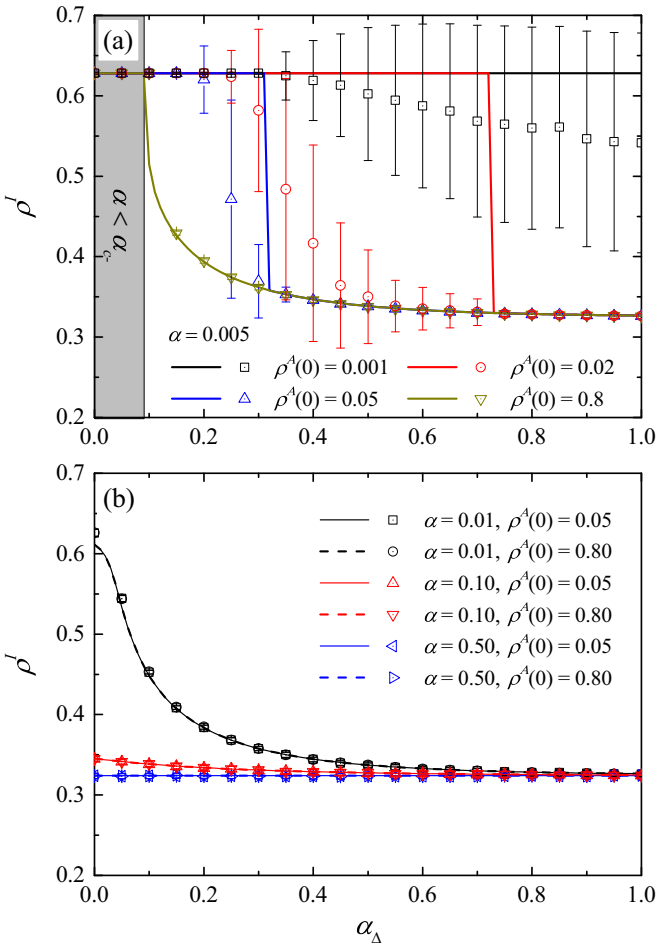

FIG. 7. The epidemic prevalence ρ^I as a function of α_Δ for different initial seeds $\rho^A(0)$ and awareness probability α. The information layer uses a RSC network with $\langle k_1 \rangle = 20$ and $\langle k_\Delta \rangle = 6$, and the epidemic layer is an ER network with $\langle k_2 \rangle = 6$. Parameters: $N = 2000$, $\kappa = 0$, $\eta = 0.3$, $\delta = 0.2$, $\beta = 0.2$, $\mu = 0.3$; (a) $\alpha = 0.005$. Lines are the theoretical estimations of Eqs. (B1)–(B5), while scatters in panels (a),(b) are simulation results obtained by averages over 1000 and 100 independent runs, respectively.

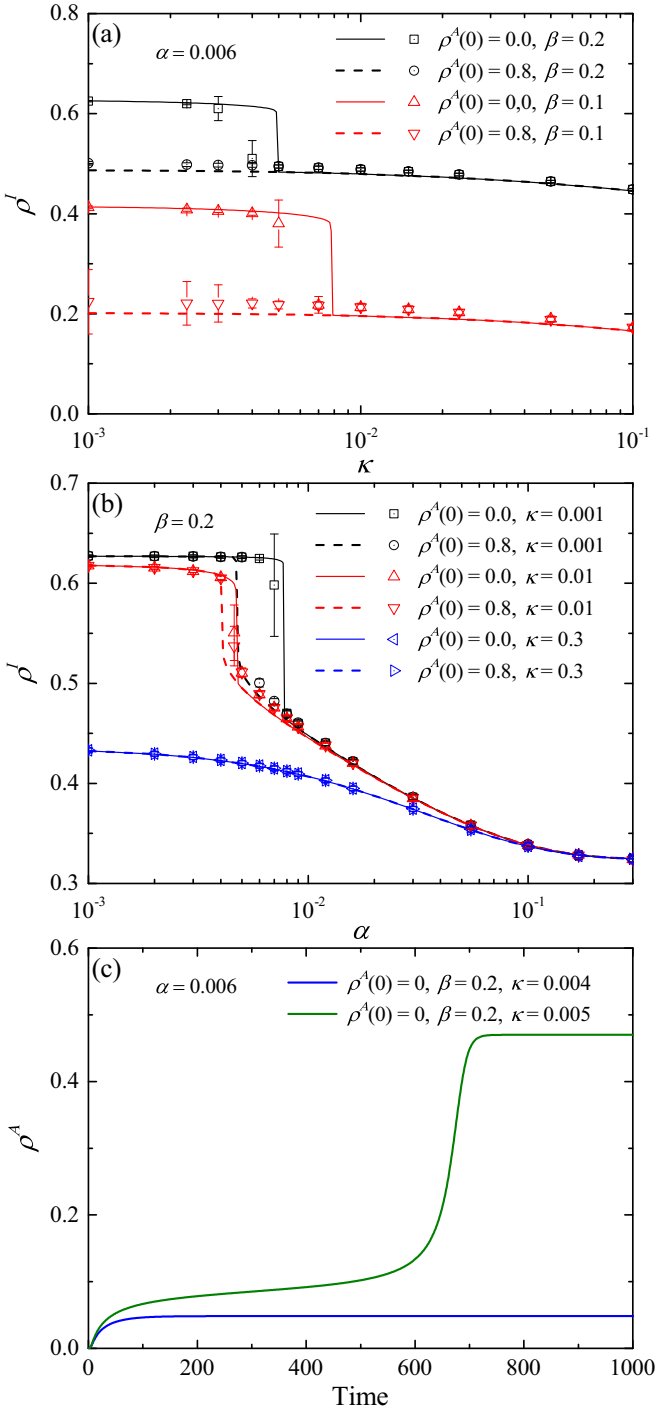

FIG. 8. The epidemic prevalence ρ^I as a function of self-awareness probability κ in panel (a) and awareness probability α in panel (b). The fractions of aware individuals as functions of time for different κ in panel (c). Parameters: $N = 2000$, $\delta = 0.2$, $\eta = 0.3$, $\alpha_\Delta = 0.1$, $\mu = 0.3$.

17% for $\alpha = 0.5$), regardless of whether or not the 2-simplices are present.

The physical nature of the initial seeds in the information layer is that these aware individuals are from external input rather than being informed by other individuals in the population. In UAU-SIS model, the self-awareness of infected individuals in the epidemic layer will also cause the external input of information layer. In Fig. 8, we discuss the effect of κ on the epidemic prevalence, where parameters α and α_Δ meet the requirements of the unshaded area of Fig. 7(a). From Fig. 8(a), one can see that the dependence of the epidemic prevalence on the initial seeds disappears suddenly with the increase of κ. In Fig. 8(b), with the increase of κ, the region that can produce bistability gradually shrinks until it disappears. When κ is not zero, the information layer may obtain aware individuals through self-awareness at any time step, which can play the role of the initial seeds. Therefore, we can see that in Fig. 8(c) the information layer always has a certain number of aware individuals. For low κ, aware individuals stabilize at a smaller proportion, which cannot activate enough 2-simplices. When κ is larger than a certain critical κ_c, a large number of 2-simplices is suddenly activated after a period of accumulation of aware individuals, and as a result the proportion of aware individuals is suddenly increased to a

high level. Here, we give an example in Fig. 8(c) to visually understand these phenomena in Figs. 8(a) and 8(b).

Moreover, Fig. 8(a) also shows that κ_c moves to the left (i.e., the smaller κ value) as the infection probability β are increased, since the external input of aware individuals is proportional to the product of κ and infected individuals. And we note that κ_c is usually very small when the parameter in the epidemic layer is far away from its threshold. Figure 8(b) shows that the increase of κ can well inhibit the disease spreading when the awareness probability α is low. And κ has no significant effect on the epidemic prevalence for high α [e.g., $\alpha > 0.1$ in Fig. 8(b)], which is consistent with the conclusion of UAU-SIS model without 2-simplices [18].

B. Time series

In the classical SIS model, the density of infected individuals converges to a constant, the endemic state, after an exponential growth [67]. However, in the epidemic layer of the UAU-SIS model, there may be an attenuation region between the exponential growth region and the endemic state, forming a peak; see Fig. 9(a). It can be clearly seen that the attenuation region of the epidemic layer is caused by the exponential growth region of the information layer. The density of infected individuals first increases rapidly to peak, then it decays because of the exponential growth of aware individuals, and finally the densities of both infected individuals and aware individuals reach their steady states. Namely, a necessary condition for the peak to occur is that the number of aware individuals on the information layer grows more slowly than the number of infected individuals on the epidemic layer. In the original UAU-SIS model without simplicial complexes (i.e., $\alpha_\Delta = 0.0$), a low diffusion speed, which is from low awareness probability α, always corresponds to a low density of aware individuals. Furthermore, the low density of aware individuals makes the peak very insignificant. Thus, a significant peak is directly caused by the 2-simplices.

Let attenuation level $\Delta\rho^I$ denote the maximum of the density of infected individuals minus the value of its steady state, i.e., $\Delta\rho^I = \rho^I(t)_{\max} - \rho^I(\infty)$. In Fig. 9(b), we plot $\Delta\rho^I$ as a function of α_Δ on the UAU-SIS model, which shows a nonmonotonic change. The reason is that the density of aware individuals and the speed of information diffusion increase simultaneously when α_Δ increases. We noticed that $\Delta\rho^I$ is only 0.0030 if the 2-simplices is excluded ($\alpha_\Delta = 0$). With the increase of α_Δ ($0 < \alpha_\Delta < 0.3$), the density of aware individuals increases, leading to the increase of $\Delta\rho^I$. The density of aware individuals is as high as 77.2% for $\alpha_\Delta = 0.3$. With the further increase of α_Δ, the increase of the speed of information diffusion makes $\Delta\rho^I$ decrease.

There are many parameters in the UAU-SIS model that can improve the speed of information diffusion. For example, the increase of initial seeds, $\rho^A(0)$, can directly accelerate the diffusion of information without changing the density of aware individuals in the steady state. The increase of awareness probability, α, can directly accelerate the diffusion of information and increase the density of aware individuals simultaneously. The increase of κ can indirectly accelerate the diffusion of information by obtaining more aware individuals through the feedback of the epidemic layer. In Fig. 10(a),

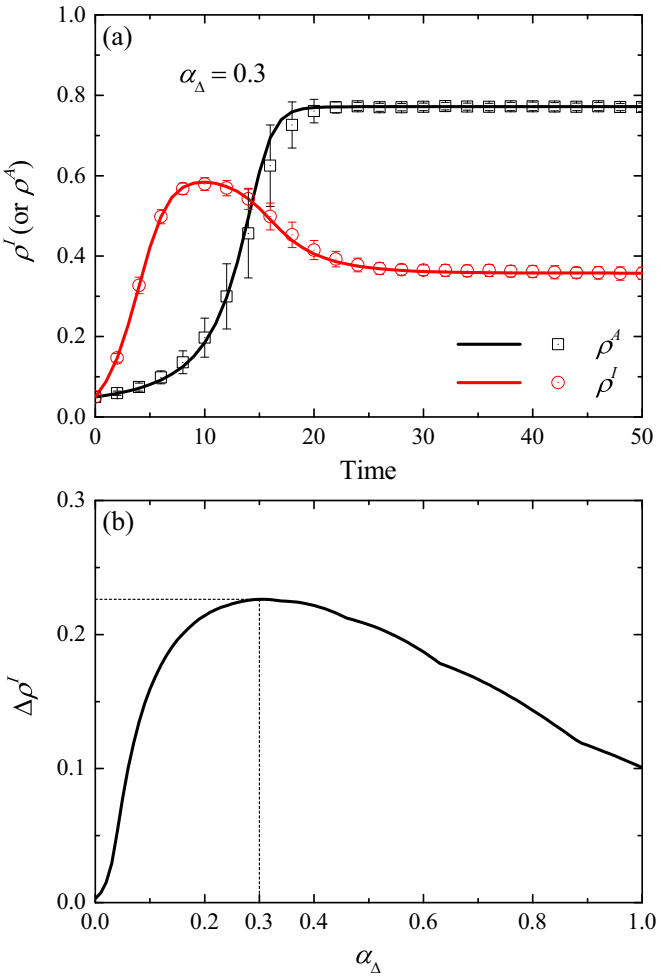

FIG. 9. (a) The fractions of aware individuals and infected individuals as functions of the time step in UAU-SIS model. (b) The attenuation level $\Delta\rho^I$ as a function of α_Δ. The information layer uses a RSC network with $\langle k_1\rangle = 20$ and $\langle k_\Delta\rangle = 6$, and the epidemic layer is an ER network with $\langle k_2\rangle = 6$. Lines are the theoretical estimations of Eqs. (B1)–(B5), while scatters in panel (a) are simulation results obtained by averages over 100 independent runs. Parameters: $N = 2000$, $\kappa = 0.0$, $\eta = 0.3$, $\delta = 0.2$, $\beta = 0.2$, $\mu = 0.3$, $\alpha = 0.01$, $\rho^A(0) = 0.05$.

there is a sudden increase in attenuation level $\Delta\rho^I$, which is the phase transition of whether a number of 2-simplices are activated, and the phase transition point moves to the left (i.e., the smaller α value) as the initial seeds $\rho^A(0)$ are increased. Meanwhile, there is also a nonmonotonic phenomenon in Fig. 10(a) under the same reason in Fig. 9(b). In Fig. 10(b), we can see that $\Delta\rho^I$ decays almost exponentially as κ increases. From Fig. 10, the increase of initial seeds makes $\Delta\rho^I$ rapidly and monotonically decrease, which is an effective way to avoid the peak in the epidemic layer.

VI. CONCLUSION

In summary, we have studied how the "complex contagion" (2-simplices) of the information layer affects the epidemic spreading in the UAU-SIS model on multiplex networks. We find that self-awareness plays a key role in epidemic threshold,

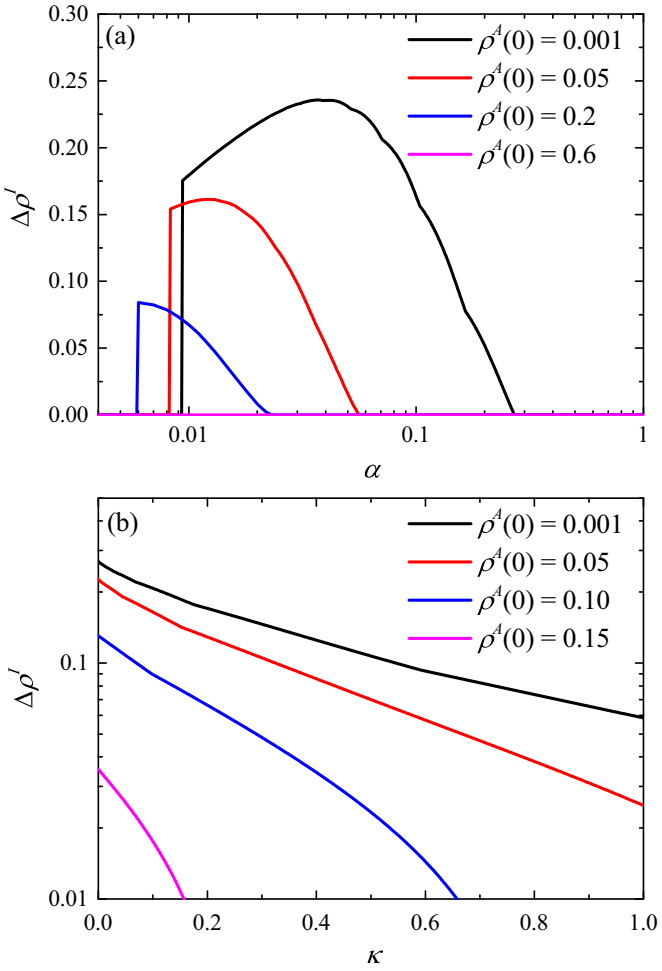

FIG. 10. The attenuation level $\Delta\rho^I$ as a function of α in panel (a) and κ in panel (b) for different initial seeds $\rho^A(0)$, respectively. The information layer uses a RSC network with $\langle k_1\rangle = 20$ and $\langle k_\Delta\rangle = 6$, and the epidemic layer is an ER network with $\langle k_2\rangle = 6$. Lines are the theoretical estimations of Eqs. (B1)–(B5). Parameters: $N = 2000$, $\eta = 0.3$, $\delta = 0.2$, $\beta = 0.2$, $\mu = 0.3$; (a) $\alpha_\Delta = 0.1$, $\kappa = 0.0$; (b) $\alpha_\Delta = 0.3$, $\alpha = 0.01$.

epidemic prevalence, and time series, which is different from the previous view.

A lot of anomalous phenomena appear around the epidemic threshold. Multiple susceptibility peaks can emerge in the susceptibility of the epidemic layer when both the 2-simplices and self-awareness are present, while the phenomenon vanishes in the case of missing 2-simplices or absent self-awareness. To be specific, there are two kinds of multiple susceptibility peaks with completely opposite mechanisms that occur in intervals $\alpha_{c-} < \alpha < \alpha_{c+}$ and $\alpha < \alpha_{c-}$, respectively. In the former, the second peak represents the epidemic threshold and the first peak is not earlier than the peak of the information layer, while the latter is completely opposite. The extra peak comes from a fluctuating migration in the information layer that does not introduce a new threshold in the epidemic layer. Finally, though the bistable phenomenon in the UAU model will migrate to the UAU-SIS model when self-awareness is absent, self-awareness can make the bistable phenomenon disappear.

For the epidemic prevalence, the increase of α_Δ can effectively inhibit the disease when α is low. Bistable phenomenon also appears in the epidemic prevalence of UAU-SIS model if self-awareness κ is absent. With the increase of κ, the region that can produce bistability gradually shrinks until it disappears. The self-awareness of infected individuals causes the external aware individuals input of information layer, which is equivalent to supplementing the initial seeds $\rho^A(0)$. As the system is far from the epidemic threshold, a small κ can make bistable phenomenon disappear.

For the time series, we find that the evolution of disease is nonmonotonic, with a peak, which is unusual in the SIS model. There are two conditions for producing a significant peak: one is that the information layer grows more slowly than the epidemic layer; the other is that the density of aware individuals is high. Thus, one basically do not see this peak until the simplicial complexes is introduced. As self-awareness κ increases, the relative height decreases almost exponentially between the peak and the steady state.

To understand the dynamics theoretically after introducing the simplicial complexes, we develop a modified heterogeneous mean-field theory for the UAU model on a single-layer network and a modified partial effective degree theory for the UAU-SIS model on multiplex networks, respectively. Furthermore, we find that the threshold relationship, which proposed in Ref. [24], between single-layer networks and multilayer networks remains valid even after considering the simplicial complexes.

To summarize, our work captures some interesting and surprising results on homogeneous multiplex networks. It is an important research line of inquiry whether the introduction of other network structures will exhibit completely different properties. Meanwhile, the study of phase transition types is also an important research line [68–71], and it is necessary to study the phase transition types of various parameters of our model. We believe our analysis will provide meaningful guidance for future research.

ACKNOWLEDGMENTS

This work was supported by the National Natural Science Foundation of China (Grants No. 11705147 and No. 11975183). Ji-Qiang Zhang and Xu-Sheng Liu were supported by the National Natural Science Foundation of China (Grant No.12165014). The authors sincerely thank the anonymous reviewers for their valuable comments that have led to the present improved version of the original manuscript.

APPENDIX A: SIMULATION PROCEDURE

There are three ways to update the state of discrete-time UAU-SIS model in the same time step, that is, the information layer is updated before the epidemic layer (UAU first), the information layer is updated after the epidemic layer (SIS first), and the two layers are updated simultaneously (Simultaneously). Here, we compare the three simulation ways in Fig. 11 and find that it has no influence on our results for the update order of states of different layers in the same time step.

For the case of "Simultaneously," the simulation procedure works as follows:

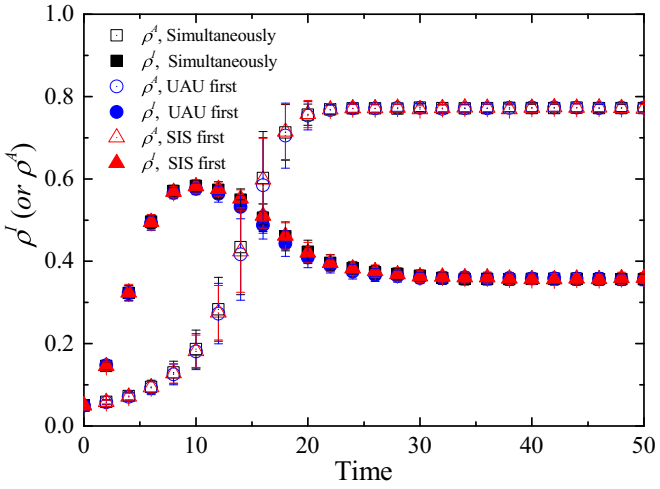

FIG. 11. The fractions of aware individuals and infected individuals as functions of the time step for three simulation ways. The information layer uses a RSC network with $\langle k_1\rangle = 20$ and $\langle k_\Delta\rangle = 6$, and the epidemic layer is an ER network with $\langle k_2\rangle = 6$. Scatters are simulation results obtained by averages over 100 independent runs. Parameters: $N = 2000$, $\kappa = 0.0$, $\eta = 0.3$, $\delta = 0.2$, $\beta = 0.2$, $\mu = 0.3$, $\alpha = 0.01$, $\alpha_\Delta = 0.3$, $\rho^A(0) = 0.05$.

Step 1: At time step t, calculate each individual's transition probabilities. The probabilities at which a US individual becomes AS, AI, UI, and US are $[1-(1-\alpha)^{n_a}(1-\alpha_\Delta)^{n_\Delta}](1-\beta)^{n_i}$, $[1-(1-\alpha)^{n_a}(1-\alpha_\Delta)^{n_\Delta}][1-(1-\beta)^{n_i}]$, $(1-\alpha)^{n_a}(1-\alpha_\Delta)^{n_\Delta}[1-(1-\beta)^{n_i}]$, $(1-\alpha)^{n_a}(1-\alpha_\Delta)^{n_\Delta}(1-\beta)^{n_i}$, respectively. Here, n_i, n_a, and n_Δ are the number of infected immediate neighbors, the number of aware immediate neighbors, and the number of 2-simplices with two other aware nodes, respectively. The probabilities at which a AS individual becomes AS, AI, UI, and US are $(1-\delta)(1-\eta\beta)^{n_i}$, $(1-\delta)[1-(1-\eta\beta)^{n_i}]$, $\delta[1-(1-\eta\beta)^{n_i}]$, $\delta(1-\eta\beta)^{n_i}$, respectively. The probabilities at which a UI individual becomes AS, AI, UI, and US are $[1-(1-\kappa)(1-\alpha)^{n_a}(1-\alpha^\Delta)^{n_\Delta}]\mu$, $[1-(1-\kappa)(1-\alpha)^{n_a}(1-\alpha^\Delta)^{n_\Delta}](1-\mu)$, $(1-\kappa)(1-\alpha)^{n_a}(1-\alpha^\Delta)^{n_\Delta}(1-\mu)$, $(1-\kappa)(1-\alpha)^{n_a}(1-\alpha^\Delta)^{n_\Delta}\mu$, respectively. The probabilities at which a AI individual becomes AS, AI, UI, and US are $(1-\delta)\mu$, $(1-\delta)(1-\mu)$, $\delta(1-\mu)$, $\delta\mu$, respectively.

Step 2: At time step $t+1$, all individuals update their states in a synchronous way according to the probabilities of Step 1.

Step 3: Repeat Steps 1–2 until the predetermined time period is reached.

For the case of "UAU first," the simulation procedure works as follows:

Step 1: At time step t, update the state of each node in the information layer by the following probabilities calculation. The probability at which a US individual becomes AS is $1-(1-\alpha)^{n_a}(1-\alpha_\Delta)^{n_\Delta}$. The probability at which a UI individual becomes AI is $1-(1-\kappa)(1-\alpha)^{n_a}(1-\alpha^\Delta)^{n_\Delta}$. The probability at which a AS individual becomes US is δ. The probability at which a AI individual becomes UI is δ.

Step 2: Update the state of each node in the epidemic layer by the following probabilities calculation. The probability at which a US individual becomes UI is $1-(1-\beta)^{n_i}$. The probability at which a AS individual becomes AI is $1-(1-\eta\beta)^{n_i}$. The probability at which a UI individual becomes US is μ. The probability at which a AI individual becomes AS is μ. Note that the updated state from Step 1 is used in this step.

Step 3: The current time step is increased by 1.

Step 4: Repeat Steps 1–3 until the predetermined time period is reached.

For the case of "SIS first," the simulation procedure works as follows:

Step 1: At time step t, update the state of each node in the epidemic layer by the following probabilities calculation. The probability at which a US individual becomes UI is $1-(1-\beta)^{n_i}$. The probability at which a AS individual becomes AI is $1-(1-\eta\beta)^{n_i}$. The probability at which a UI individual becomes US is μ. The probability at which a AI individual becomes AS is μ.

Step 2: Update the state of each node in the information layer by the following probabilities calculation. The probability at which a US individual becomes AS is $1-(1-\alpha)^{n_a}(1-\alpha_\Delta)^{n_\Delta}$. The probability at which a UI individual becomes AI is $1-(1-\kappa)(1-\alpha)^{n_a}(1-\alpha^\Delta)^{n_\Delta}$. The probability at which a AS individual becomes US is δ. The probability at which a AI individual becomes UI is δ. Note that the updated state from Step 1 is used in this step.

Step 3: The current time step is increased by 1.

Step 4: Repeat Steps 1–3 until the predetermined time period is reached.

APPENDIX B: MODIFIED DISCRETE-TIME PARTIAL EFFECTIVE DEGREE THEORY ON UAU-SIS MODEL WITH SIMPLICIAL COMPLEXES

Here, we modify partial effective degree theory [21,24] to accommodate the introduction of simplicial complexes. Specifically, the information layer uses the modified heterogeneous mean-field theory in Sec. III and the epidemic layer adopts the effective degree theory in Ref. [65]. As a result, individuals are classified as $X_{k_1,k_\Delta}Y_{s,i}$, where $X \in \{U, A\}$ and $Y \in \{S, I\}$. The subscripts k_1 and k_Δ are the number of neighbors and 2-simplexes in the information layer for a selected individual, and the subscripts s and i denote the number of its susceptible and infected neighbors in the epidemic layer, where $s+i=k_2$. Note that $X_{k_1,k_\Delta}Y_{s,i}(t)$ is also used to denote the fraction of individuals in corresponding states at the time step t. For the sake of clarity and convenience, all possible state transitions of individuals at each time step are shown in Fig. 12.

In the information layer, we use $H_{U\to A,S}$ (or $H_{U\to A,I}$) to denote the probability that an unaware individual in class $U_{k_1,k_\Delta}S_{m,n}$ (or $U_{k_1,k_\Delta}I_{m,n}$) becomes an aware individual during the next time step. Considering pairwise interactions, 2-simplices, and self-awareness, we have

$$\begin{aligned} H_{U\to A,S} &= 1-(1-\alpha\varphi)^{k_1}(1-\alpha_\Delta\varphi^2)^{k_\Delta}, \\ H_{U\to A,I} &= 1-(1-\alpha\varphi)^{k_1}(1-\alpha_\Delta\varphi^2)^{k_\Delta}(1-\kappa), \end{aligned} \quad \text{(B1)}$$

where φ is the probability of an unaware individual in contact with any aware individual (corresponding to ϕ in Sec. III), and

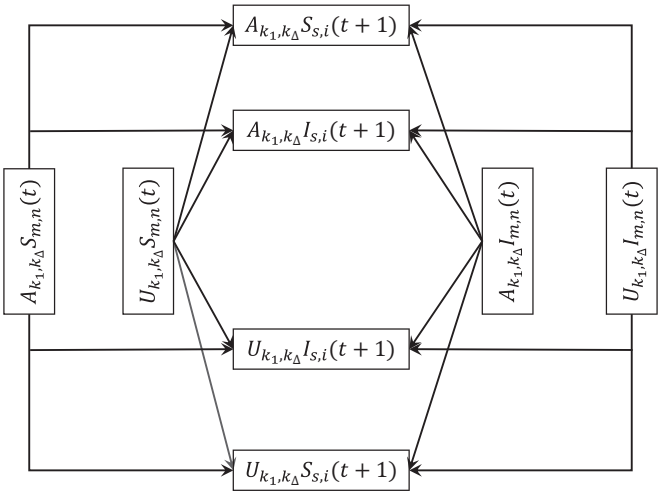

FIG. 12. Schematic illustration of the transition of the whole classes at one time step, where $m+n=s+i$.

its value can be calculated by

$$\varphi = \frac{\sum_{k_1,k_\Delta,m,n} k_1\left(A_{k_1,k_\Delta}S_{m,n} + A_{k_1,k_\Delta}I_{m,n}\right)}{\sum_{k_1,k_\Delta} k_1 P_1(k_1,k_\Delta)}.$$

In the epidemic layer, we use $H_{U,S\to I}$ (or $H_{A,S\to I}$) to denote the probability that a susceptible individual in class $U_{k_1,k_\Delta}S_{m,n}$ (or $A_{k_1,k_\Delta}S_{m,n}$) becomes an infected individual during the next time step. Considering pairwise interaction and self-protection, we have

$$\begin{aligned} H_{U,S\to I} &= 1-(1-\beta)^n, \\ H_{A,S\to I} &= 1-(1-\eta\beta)^n. \end{aligned} \tag{B2}$$

In effective degree theory, changes in individual states and in its subscripts occur simultaneously. We use $F_{S,m\to s}$ to denote the probability of the subscript transformation from $X_{k_1,k_\Delta}S_{m,n}$ to $X_{k_1,k_\Delta}S_{s,m+n-s}$, and $F_{I,m\to s}$ to denote the probability of the subscript transformation from $X_{k_1,k_\Delta}I_{m,n}$ to $X_{k_1,k_\Delta}I_{s,m+n-s}$. Let p be the number of infected individuals recovered, we have

$$\begin{aligned} F_{S,m\to s} &= \sum_{p=\max\{0,s-m\}}^{\min\{s,n\}} \left[\binom{n}{p}\mu^p(1-\mu)^{n-p} \times \binom{m}{p-s+m} G_S^{p-s+m}(1-G_S)^{s-p}\right], \\ F_{I,m\to s} &= \sum_{p=\max\{0,s-m\}}^{\min\{s,n\}} \left[\binom{n}{p}\mu^p(1-\mu)^{n-p} \times \binom{m}{p-s+m} G_I^{p-s+m}(1-G_I)^{s-p}\right], \end{aligned} \tag{B3}$$

where G_S and G_I are the probabilities that a susceptible neighbor of susceptible and infected individuals becomes an infected neighbor during the next time step, and their values are calculated by

$$\begin{aligned} G_S &= \frac{\sum_{k_1,k_\Delta,m,n} m\left(A_{k_1,k_\Delta}S_{m,n}H_{A,S\to I} + U_{k_1,k_\Delta}S_{m,n}H_{U,S\to I}\right)}{\sum_{k_1,k_\Delta,m,n} m\left(U_{k_1,k_\Delta}S_{m,n} + A_{k_1,k_\Delta}S_{m,n}\right)}, \\ G_I &= \frac{\sum_{k_1,k_\Delta,m,n} n\left(A_{k_1,k_\Delta}S_{m,n}H_{A,S\to I} + U_{k_1,k_\Delta}S_{m,n}H_{U,S\to I}\right)}{\sum_{k_1,k_\Delta,m,n} n\left(U_{k_1,k_\Delta}S_{m,n} + A_{k_1,k_\Delta}S_{m,n}\right)}. \end{aligned}$$

According to Eqs. (B1)–(B3), the modified discrete-time partial effective degree Markov chain equations for the UAU-SIS model are shown as follows:

$$\begin{aligned} A_{k_1,k_\Delta}S_{s,i}(t+1) = \sum_{m+n=s+i} \Big\{ & (1-\delta)(1-H_{A,S\to I})F_{S,m\to s}A_{k_1,k_\Delta}S_{m,n}(t) + H_{U\to A,S}(1-H_{U,S\to I})F_{S,m\to s}U_{k_1,k_\Delta}S_{m,n}(t) \\ & + (1-\delta)\mu F_{I,m\to s}A_{k_1,k_\Delta}I_{m,n}(t) + H_{U\to A,I}\mu F_{I,m\to s}U_{k_1,k_\Delta}I_{m,n}(t)\Big\}, \\ A_{k_1,k_\Delta}I_{s,i}(t+1) = \sum_{m+n=s+i} \Big\{ & (1-\delta)H_{A,S\to I}F_{S,m\to s}A_{k_1,k_\Delta}S_{m,n}(t) + H_{U\to A,S}H_{U,S\to I}F_{S,m\to s}U_{k_1,k_\Delta}S_{m,n}(t) \\ & + (1-\delta)(1-\mu)F_{I,m\to s}A_{k_1,k_\Delta}I_{m,n}(t) + H_{U\to A,I}(1-\mu)F_{I,m\to s}U_{k_1,k_\Delta}I_{m,n}(t)\Big\}, \\ U_{k_1,k_\Delta}I_{s,i}(t+1) = \sum_{m+n=s+i} \Big\{ & \delta H_{A,S\to I}F_{S,m\to s}A_{k_1,k_\Delta}S_{m,n}(t) + (1-H_{U\to A,S})H_{U,S\to I}F_{S,m\to s}U_{k_1,k_\Delta}S_{m,n}(t) \\ & + \delta(1-\mu)F_{I,m\to s}A_{k_1,k_\Delta}I_{m,n}(t) + (1-H_{U\to A,I})(1-\mu)F_{I,m\to s}U_{k_1,k_\Delta}I_{m,n}(t)\Big\}, \\ U_{k_1,k_\Delta}S_{s,i}(t+1) = \sum_{m+n=s+i} \Big\{ & \delta(1-H_{A,S\to I})F_{S,m\to s}A_{k_1,k_\Delta}S_{m,n}(t) + (1-H_{U\to A,S})(1-H_{U,S\to I})F_{S,m\to s}U_{k_1,k_\Delta}S_{m,n}(t) \\ & + \delta\mu F_{I,m\to s}A_{k_1,k_\Delta}I_{m,n}(t) + (1-H_{U\to A,I})\mu F_{I,m\to s}U_{k_1,k_\Delta}I_{m,n}(t)\Big\}. \end{aligned} \tag{B4}$$

Finally, the fractions of aware individuals and infected individuals in UAU-SIS model at time step t are calculated by

$$\rho^I(t) = \sum_{k_1,k_\Delta,s,i} \left[U_{k_1,k_\Delta} I_{s,i}(t) + A_{k_1,k_\Delta} I_{s,i}(t)\right], \quad \rho^A(t) = \sum_{k_1,k_\Delta,s,i} \left[A_{k_1,k_\Delta} S_{s,i}(t) + A_{k_1,k_\Delta} I_{s,i}(t)\right]. \tag{B5}$$

In Secs. V A and V B, we show that the numerical solutions of the partial validity theory are consistent with the Monte Carlo simulation results in both time series and epidemic prevalence.

[1] N. Ferguson, Capturing human behaviour, Nature **446**, 733 (2007).

[2] H.-F. Zhang, J.-R. Xie, M. Tang, and Y.-C. Lai, Suppression of epidemic spreading in complex networks by local information based behavioral responses, Chaos **24**, 043106 (2014).

[3] X.-X. Zhan, C. Liu, G. Zhou, Z.-K. Zhang, G.-Q. Sun, and J. J. Zhu, Mutual feedback between epidemic spreading and information diffusion, arXiv:1506.03932.

[4] S. Funk, E. Gilad, C. Watkins, and V. A. A. Jansen, The spread of awareness and its impact on epidemic outbreaks, Proc. Natl. Acad. Sci. USA **106**, 6872 (2009).

[5] S. Funk, E. Gilad, and V. Jansen, Endemic disease, awareness, and local behavioural response, J. Theor. Biol. **264**, 501 (2010).

[6] I. Z. Kiss, J. Cassell, M. Recker, and P. L. Simon, The impact of information transmission on epidemic outbreaks, Math. Biosci. **225**, 1 (2010).

[7] Q. Wu, X. Fu, M. Small, and X.-J. Xu, The impact of awareness on epidemic spreading in networks, Chaos **22**, 013101 (2012).

[8] Z. Wang, M. A. Andrews, Z.-X. Wu, L. Wang, and C. T. Bauch, Coupled disease-behavior dynamics on complex networks: A review, Phys. Life Rev. **15**, 1 (2015).

[9] X.-X. Zhan, C. Liu, G.-Q. Sun, and Z.-K. Zhang, Epidemic dynamics on information-driven adaptive networks, Chaos, Soliton. Fract. **108**, 196 (2018).

[10] Z.-K. Zhang, C. Liu, X.-X. Zhan, X. Lu, C.-X. Zhang, and Y.-C. Zhang, Dynamics of information diffusion and its applications on complex networks, Phys. Rep. **651**, 1 (2016).

[11] D. Notarmuzi, C. Castellano, A. Flammini, D. Mazzilli, and F. Radicchi, Universality, criticality and complexity of information propagation in social media, Nat. Commun. **13**, 1308 (2022).

[12] S. Gómez, A. Díaz-Guilera, J. Gómez-Gardeñes, C. J. Pérez-Vicente, Y. Moreno, and A. Arenas, Diffusion Dynamics on Multiplex Networks, Phys. Rev. Lett. **110**, 028701 (2013).

[13] M. De Domenico, C. Granell, M. A. Porter, and A. Arenas, The physics of spreading processes in multilayer networks, Nat. Phys. **12**, 901 (2016).

[14] G. F. de Arruda, E. Cozzo, T. P. Peixoto, F. A. Rodrigues, and Y. Moreno, Disease Localization in Multilayer Networks, Phys. Rev. X **7**, 011014 (2017).

[15] G. Bianconi, *Multilayer Networks: Structure and Function* (Oxford University Press, Oxford, UK, 2018).

[16] E. Cozzo, G. F. De Arruda, F. A. Rodrigues, and Y. Moreno, *Multiplex Networks: Basic Formalism and Structural Properties* (Springer International Publishing, Berlin, 2018).

[17] C. Granell, S. Gómez, and A. Arenas, Dynamical Interplay between Awareness and Epidemic Spreading in Multiplex Networks, Phys. Rev. Lett. **111**, 128701 (2013).

[18] C. Granell, S. Gómez, and A. Arenas, Competing spreading processes on multiplex networks: Awareness and epidemics, Phys. Rev. E **90**, 012808 (2014).

[19] J.-Q. Kan and H.-F. Zhang, Effects of awareness diffusion and self-initiated awareness behavior on epidemic spreading—An approach based on multiplex networks, Commun. Nonlin. Sci. Numer. Simul. **44**, 193 (2017).

[20] Y. Pan and Z. Yan, The impact of multiple information on coupled awareness-epidemic dynamics in multiplex networks, Physica A **491**, 45 (2018).

[21] Y. Zhou, J. Zhou, G. Chen, and H. E. Stanley, Effective degree theory for awareness and epidemic spreading on multiplex networks, New J. Phys. **21**, 035002 (2019).

[22] Paulo Cesar Ventura da Silva, F. Velásquez-Rojas, C. Connaughton, F. Vazquez, Y. Moreno, and F. A. Rodrigues, Epidemic spreading with awareness and different timescales in multiplex networks, Phys. Rev. E **100**, 032313 (2019).

[23] F. Velásquez-Rojas, P. C. Ventura, C. Connaughton, Y. Moreno, F. A. Rodrigues, and F. Vazquez, Disease and information spreading at different speeds in multiplex networks, Phys. Rev. E **102**, 022312 (2020).

[24] X. Chang, C.-R. Cai, J.-Q. Zhang, and C.-Y. Wang, Analytical solution of epidemic threshold for coupled information-epidemic dynamics on multiplex networks with alterable heterogeneity, Phys. Rev. E **104**, 044303 (2021).

[25] X. Wang, X. Zhu, X. Tao, J. Xiao, W. Wang, and Y.-C. Lai, Anomalous role of information diffusion in epidemic spreading, Phys. Rev. Res. **3**, 013157 (2021).

[26] Z. Wang, C. Xia, Z. Chen, and G. Chen, Epidemic propagation with positive and negative preventive information in multiplex networks, IEEE Trans. Cybern. **51**, 1454 (2021).

[27] C. Xia, Z. Wang, C. Zheng, Q. Guo, Y. Shi, M. Dehmer, and Z. Chen, A new coupled disease-awareness spreading model with mass media on multiplex networks, Inf. Sci. **471**, 185 (2019).

[28] M. Sun, Y. Tao, and X. Fu, Asymmetrical dynamics of epidemic propagation and awareness diffusion in multiplex networks, Chaos **31**, 093134 (2021).

[29] Z. Li, P. Zhu, D. Zhao, Z. Deng, and Z. Wang, Suppression of epidemic spreading process on multiplex networks via active immunization, Chaos **29**, 073111 (2019).

[30] R. M. Anderson and R. M. May, *Infectious Diseases of Humans: Dynamics and Control* (Oxford University Press, Oxford, UK, 1991).

[31] A. Barrat, M. Barthélemy, and A. Vespignani, *Dynamical Processes on Complex Networks* (Cambridge University Press, Cambridge, UK, 2008).

[32] D. Centola and M. Macy, Complex contagions and the weakness of long ties, Am. J. Sociol. **113**, 702 (2007).

[33] D. Centola, The spread of behavior in an online social network experiment, Science **329**, 1194 (2010).

[34] M. Karsai, G. Iñiguez, K. Kaski, and J. Kertész, Complex contagion process in spreading of online innovation, J. R. Soc. Interface **11**, 20140694 (2014).

[35] P. Cui, M. Tang, and Z.-X. Wu, Message spreading in networks with stickiness and persistence: Large clustering does not always facilitate large-scale diffusion, Sci. Rep. **4**, 6303 (2014).

[36] L. Hébert-Dufresne, S. V. Scarpino, and J.-G. Young, Macroscopic patterns of interacting contagions are indistinguishable from social reinforcement, Nat. Phys. **16**, 426 (2020).

[37] D. Centola, *How Behavior Spreads* (Princeton University Press, Princeton, NJ, 2018).

[38] S. Lehmann and Y.-Y. Ahn, *Complex Spreading Phenomena in Social Systems: Influence and Contagion in Real-World Social Networks* (Springer, Berlin, 2018).

[39] A. R. Benson, D. F. Gleich, and J. Leskovec, Higher-order organization of complex networks, Science **353**, 163 (2016).

[40] F. Battiston, G. Cencetti, I. Iacopini, V. Latora, M. Lucas, A. Patania, J.-G. Young, and G. Petri, Networks beyond pairwise interactions: Structure and dynamics, Phys. Rep. **874**, 1 (2020).

[41] F. Battiston, E. Amico, A. Barrat, G. Bianconi, G. Ferraz de Arruda, B. Franceschiello, I. Iacopini, S. Kéfi, V. Latora, Y. Moreno *et al.*, The physics of higher-order interactions in complex systems, Nat. Phys. **17**, 1093 (2021).

[42] G. Bianconi, *Higher Order Networks: An Introduction to Simplicial Complexes* (Cambridge University Press, Cambridge, UK, 2021).

[43] F. E. Rosas, P. A. Mediano, A. I. Luppi, T. F. Varley, J. T. Lizier, S. Stramaglia, H. J. Jensen, and D. Marinazzo, Disentangling high-order mechanisms and high-order behaviours in complex systems, Nat. Phys.,**18**, 476 (2022).

[44] S. Majhi, M. Perc, and D. Ghosh, Dynamics on higher-order networks: A review, J. R. Soc. Interface **19**, 20220043 (2022).

[45] M. Kahle, Topology of random simplicial complexes: A survey, AMS Contemp. Math **620**, 201 (2014).

[46] O. T. Courtney and G. Bianconi, Generalized network structures: The configuration model and the canonical ensemble of simplicial complexes, Phys. Rev. E **93**, 062311 (2016).

[47] A. Costa and M. Farber, Random simplicial complexes, *Configuration Spaces* (Springer, Cham, 2016), pp. 129–153.

[48] J.-G. Young, G. Petri, F. Vaccarino, and A. Patania, Construction of and efficient sampling from the simplicial configuration model, Phys. Rev. E **96**, 032312 (2017).

[49] C. Berge, *Graphs and Hypergraphs* (North-Holland Publishing, Amsterdam, 1973).

[50] G. F. de Arruda, G. Petri, and Y. Moreno, Social contagion models on hypergraphs, Phys. Rev. Res. **2**, 023032 (2020).

[51] B. Jhun, Effective epidemic containment strategy in hypergraphs, Phys. Rev. Res. **3**, 033282 (2021).

[52] J. T. Matamalas, S. Gómez, and A. Arenas, Abrupt phase transition of epidemic spreading in simplicial complexes, Phys. Rev. Res. **2**, 012049(R) (2020).

[53] I. Iacopini, G. Petri, A. Barrat, and V. Latora, Simplicial models of social contagion, Nat. Commun. **10**, 2485 (2019).

[54] S. Chowdhary, A. Kumar, G. Cencetti, I. Iacopini, and F. Battiston, Simplicial contagion in temporal higher-order networks, J. Phys. Complex. **2**, 035019 (2021).

[55] D. Wang, Y. Zhao, J. Luo, and H. Leng, Simplicial sirs epidemic models with nonlinear incidence rates, Chaos **31**, 053112 (2021).

[56] G. St-Onge, H. Sun, A. Allard, L. Hébert-Dufresne, and G. Bianconi, Universal Nonlinear Infection Kernel from Heterogeneous Exposure on Higher-Order Networks, Phys. Rev. Lett. **127**, 158301 (2021).

[57] M. Lucas, G. Cencetti, and F. Battiston, Multiorder laplacian for synchronization in higher-order networks, Phys. Rev. Res. **2**, 033410 (2020).

[58] C. W. Lynn and D. S. Bassett, The physics of brain network structure, function and control, Nat. Rev. Phys. **1**, 318 (2019).

[59] E. Bairey, E. D. Kelsic, and R. Kishony, High-order species interactions shape ecosystem diversity, Nat. Commun. **7**, 12285 (2016).

[60] P. Erdős and A. Rényi, On random graphs I, Publ. Math. Debrecen **6**, 290 (1959).

[61] R. Pastor-Satorras and A. Vespignani, Epidemic Spreading in Scale-Free Networks, Phys. Rev. Lett. **86**, 3200 (2001).

[62] S. C. Ferreira, C. Castellano, and R. Pastor-Satorras, Epidemic thresholds of the susceptible-infected-susceptible model on networks: A comparison of numerical and theoretical results, Phys. Rev. E **86**, 041125 (2012).

[63] S. Gómez, A. Arenas, J. Borge-Holthoefer, S. Meloni, and Y. Moreno, Discrete-time Markov chain approach to contact-based disease spreading in complex networks, Europhys. Lett. **89**, 38009 (2010).

[64] J. T. Matamalas, A. Arenas, and S. Gómez, Effective approach to epidemic containment using link equations in complex networks, Sci. Adv. **4**, eaau4212 (2018).

[65] C.-R. Cai, Z.-X. Wu, and J.-Y. Guan, Effective degree Markov-chain approach for discrete-time epidemic processes on uncorrelated networks, Phys. Rev. E **90**, 052803 (2014).

[66] X. Chang and C.-R. Cai, Analytical computation of the epidemic prevalence and threshold for the discrete-time susceptible-infected-susceptible dynamics on static networks, Physica A **571**, 125850 (2021).

[67] R. Pastor-Satorras, C. Castellano, P. Van Mieghem, and A. Vespignani, Epidemic processes in complex networks, Rev. Mod. Phys. **87**, 925 (2015).

[68] G. F. de Arruda, G. Petri, P. M. Rodriguez, and Y. Moreno, Multistability, intermittency and hybrid transitions in social contagion models on hypergraphs, Nat. Commun. **14**, 1375 (2023).

[69] J. Park, S. Yi, and B. Kahng, Hysteresis and criticality in hybrid percolation transitions, Chaos **30**, 051102 (2020).

[70] X. Chen, R. Wang, M. Tang, S. Cai, H. E. Stanley, and L. A. Braunstein, Suppressing epidemic spreading in multiplex networks with social-support, New J. Phys. **20**, 013007 (2018).

[71] P. Grassberger, L. Chen, F. Ghanbarnejad, and W. Cai, Phase transitions in cooperative coinfections: Simulation results for networks and lattices, Phys. Rev. E **93**, 042316 (2016).